Complex polarization-phase and spatial-frequency selections of laser images of blood-plasma films in diagnostics of changes in their polycrystalline structure

8 AUTHORS, INCLUDING:

Yu. A. Ushenko
Chernivtsi National University
140 PUBLICATIONS **824** CITATIONS

Ozar Mintser
Shupyk National Medical Academy Of Postgr…
765 PUBLICATIONS **13** CITATIONS

GEOMETRICAL
AND APPLIED OPTICS

Complex Polarization–Phase and Spatial-Frequency Selections of Laser Images of Blood-Plasma Films in Diagnostics of Changes in Their Polycrystalline Structure

Yu. A. Ushenko[a], P. O. Angelskii[b], A. V. Dubolazov[b], A. O. Karachevtsev[b],
M. I. Sidor[b], O. P. Mintser[b], B. P. Oleinichenko[b], and L. I. Bizer[b]

[a] *Yuriy Fedkovych Chernivtsi National University, Department of Correlation and Spectroscopy, Chernivtsi, 58012 Ukraine*
[b] *Yuriy Fedkovych Chernivtsi National University, Department of Optics and Spectroscopy, Chernivtsi, 58012 Ukraine*
e-mail: yuriyu@gmail.com

Abstract—We present a theoretical formalism of correlation phase analysis of laser images of human blood plasma with spatial-frequency selection of manifestations of mechanisms of linear and circular birefringence of albumin and globulin polycrystalline networks. Comparative results of the measurement of coordinate distributions of the correlation parameter—the modulus of the degree of local correlation of amplitudes—of laser images of blood plasma taken from patients of three groups—healthy patients (donors), rheumatoid-arthritis patients, and breast-cancer patients—are presented. We investigate values and ranges of change of statistical (the first to fourth statistical moments), correlation (excess of autocorrelation functions), and fractal (slopes of approximating curves and dispersion of extrema of logarithmic dependences of power spectra) parameters of coordinate distributions of the degree of local correlation of amplitudes. Objective criteria for diagnostics of occurrence and differentiation of inflammatory and oncological states are determined.

INTRODUCTION

Among the various areas of optical diagnostics of biological objects [1−12], an independent area—laser polarimetry of distributions of the azimuth and ellipticity of polarization of images of polycrystalline structures of human tissues and liquids—has been singled out [13−17]. A generalization of this approach became a new "two-point" analysis of the polarization structure of these fields. This direction, which was proposed and developed in a series of theoretical [18−21] and applied [22−24] investigations, is based on the use of new correlation parameters for the description of mutual relations between coordinate structures of optically anisotropic protein networks (complex degree of mutual anisotropy (CDMA)) and their polarization inhomogeneous laser images (complex degree of mutual polarization (CDMP)). At the same time, the theoretical ground that was used of polarization correlometry, which is based on the approximation of only linear birefringence of biological layers [25−29], should also take into account other mechanisms of anisotropy (optical activity, dichroism). In addition, it is important to develop methods for processing images of biological objects with a weak optical anisotropy. In this case, polarization modulation is insignificant and extraction of phase information proves to be important. One of the parameters that can be used to analyze these images is the degree of local

correlation of amplitudes (DLCA), which was introduced for the first time in theoretical investigations [19, 20].

The objective of this work is to develop and test a method for the selection of distributions of the parameter DLCA of laser images of blood-plasma films using coordinated polarization–phase and Fourier filtration for diagnostics of changes in their polycrystalline structure caused by inflammatory and oncological changes in human organs.

BRIEF THEORY OF THE METHOD

Traditionally, structures of histological sections of biological tissues and films of biological liquids are studied by visual-microscopy methods. There are various methods for increasing contrast and selecting microscopic images. Among them, one can single out structural (dark-field method) and phase (phase-contrast method) techniques. Using the dark-field method [30, 31], one cannot determine variations in the refractive index of visualized structural elements. This information can be provided by the phase-contrast method [32, 33]. In the obtained image of a biological specimen, the intensity distribution reproduces the phase relief. At the same time, this approach cannot distinguish between different mechanisms of phase anisotropy—linear birefringence and optical activity of elements of the biological layer.

Let us consider the possibility of selection of these mechanisms using a complex polarization–phase and spatial-frequency analyses of microscopic images.

As a basis for analysis of the formation of a laser-radiation field, we will use the model of optically anisotropic albumin and globulin networks that was proposed in [29, 34–37].

Needle-shaped albumin crystals are large-scale (their length is 50–100 μm) and possess a linear birefringence. Spheroidal optically active crystals are small-scale (their diameter is 5–20 μm).

The optical anisotropy of these networks is characterized by the Jones matrix

$$\{D\} = \left\| \begin{array}{cc} [\sin^2\rho + \cos^2\rho\,\exp(-i\delta)] & [\sin\rho\cos\rho(1-\exp(-i\delta))] \\ [\sin\rho\cos\rho(1-\exp(-i\delta))] & [\cos^2\rho + \sin^2\rho\,\exp(-i\delta)] \end{array} \right\| \times \left\| \begin{array}{cc} \cos\theta & \sin\theta \\ -\sin\theta & \cos\theta \end{array} \right\|.$$

Here, ρ is the angle between the plane of incidence of the radiation and the direction of the optical axis of crystals (fibrils) in the plane of the specimen; $\delta = (2\pi/\lambda)\Delta nl$ is the magnitude of the phase shift between the orthogonal components of the laser-radiation field with the wavelength λ, which traveled along geometric path l through the biological crystal with the birefringence Δn; and θ is the angle of rotation of the plane of polarization of the laser wave.

The two-point correlation–phase method of investigation of the polycrystalline structure of blood-plasma films is based on the notion of the degree of local correlation of amplitudes (DLCA) [20].

In the general case, this parameter, which is denoted as $\mu(r_1, r_2)$, characterizes the mutual correlation between the orthogonal components of the amplitude (E_x, E_y) of the laser field at two points with coordinates r_1 and r_2,

$$\mu(r_1, r_2) = \left[\frac{\mathrm{Tr}(W^{\diamond}(r_1, r_2)W(r_1, r_2))}{\mathrm{Tr}\,W(r_1, r_1)\mathrm{Tr}\,W(r_2, r_2)} \right]. \quad (1)$$

Here, $W(r_1, r_2)$ is the transversally spectral density matrix of the following form:

$$W(r_1, r_2) = \begin{bmatrix} E_x^*(r_1)E_x(r_2) & E_x^*(r_1)E_y(r_2) \\ E_y^*(r_1)E_x(r_2) & E_y^*(r_1)E_y(r_2) \end{bmatrix}, \quad (2)$$

where $W^{\diamond}(r_1, r_2)$ is the matrix that is Hermitian conjugate to $W(r_1, r_2)$ and Tr is the trace of the matrix.

We will write expression (1) for the laser field transformed by the protein crystal at its two arbitrary points. In this case, the transversally spectral density matrix (relation (2)) of this field takes the form

$$W_{\mathrm{out}}(r_1, r_2) = D^{\diamond}(r_1)W_{\mathrm{in}}(r_1, r_2)D(r_2). \quad (3)$$

Here, $D(r_1)$ and $D(r_2)$ are the Jones matrices of the crystal at points r_1 and r_2, and $W_{\mathrm{in}}(x_1, x_2)$ is the transversally spectral density matrix of the probing laser beam,

$$W_{\mathrm{in}}(r_1, r_2) = \begin{bmatrix} E_x^*(r_1)E_x(r_2) & E_x^*(r_1)E_y(r_2) \\ E_y^*(r_1)E_x(r_2) & E_y^*(r_1)E_y(r_2) \end{bmatrix}. \quad (4)$$

Let us determine the analytical form of the DLCA for the case of probing of a protein crystal by a plane polarized laser wave with the azimuth 0,

$$E_0 = \begin{pmatrix} E_{0x}\exp(-i\varphi_{0x}) \\ E_{0y}\exp(-i\varphi_{0y}) \end{pmatrix} \rightarrow E_0(0) = \begin{pmatrix} 1 \\ 0 \end{pmatrix}.$$

Taking into account the smallness of the birefringence index and optical activity (Δn, $\Delta n^* \sim 10^{-3}$), as well as small transverse size ($l \sim 5-10$ μm) of albumin and globulin, in what follows, we restrict ourselves to the approximation of a weak anisotropy [38]. In this case, the values of phase shift δ and angle of rotation of the plane of polarization θ of the laser wave are rather small, $\delta \approx \theta \le 0.14$ rad. Therefore, we can assume that $\begin{cases} \sin\delta \approx \delta, \sin\theta \approx \theta, \\ \cos\delta \approx \cos\theta \rightarrow 1 \end{cases}$. Under these conditions, the orthogonal components of Jones vector $E = \begin{pmatrix} E_x\exp(-i\varphi_x) \\ E_y\exp(-i\varphi_y) \end{pmatrix}$ of the object wave are determined by the following relations:

$$\begin{cases} E_x(0) = 1 - i\delta\cos\rho\,(\cos\rho + \theta\sin\rho), \\ E_y(0) = \theta - i\delta\sin\rho\,(\cos\rho + \theta\sin\rho). \end{cases} \quad (5)$$

Taking into account relations (4)–(10), the expression for the DLCA of two points of the laser image of the blood-plasma film takes the form

$$\mu(r_1, r_2) = \sqrt{\frac{1}{(a+ib)(\cos^2\Delta\rho_{12}\cos\Delta\theta_{12} + \sin^2\Delta\rho_{12}\sin\Delta\theta_{12}\exp(-i2\Delta\delta_{12}))}}. \quad (6)$$

Here, $\Delta\rho_{12} = \rho(r_1) - \rho(r_2)$, $\Delta\delta_{12} = \delta(r_1) - \delta(r_2)$, and $\Delta\theta_{12} = \theta(r_1) - \theta(r_2)$ are the "difference" orientational and phase structures of the parameter of the polycrystalline network at points with coordinates r_1 and r_2, $a + ib$ is the proportionality coefficient.

Analysis of expression (6) reveals that DLCA depends on both the orientational ($\Delta\rho$) and phase ($\Delta\delta$, $\Delta\theta$) structures of the polycrystalline network of proteins of the blood-plasma film. This ambiguity can be eliminated by probing with a circularly polarized beam. In this case, expression (6) is transformed into the phase dependence alone,

$$\mu(r_1, r_2) = \sqrt{\frac{1}{(\exp(-i2\Delta\delta_{12})\sin\Delta\theta_{12} + \cos\Delta\theta_{12})}}. \quad (7)$$

Below, we will take into account only the modulus of CKRF, the value of which can be measured experimentally,

$$|\mu(r_1, r_2)| = (1 + 2\Delta\delta_{12}\Delta\theta_{12})^{-1}. \quad (8)$$

Therefore, to determine the value of $|\mu(r_1, r_2)|$, it is necessary to know the difference of the phase shifts between the orthogonal components of amplitudes $E_x(r_1)$, $E_y(r_1)$ and $E_x(r_2)$, $E_y(r_2)$ at the points with coordinates r_1 and r_2, which are formed both by linear birefringence $\delta(r_1) - \delta(r_2)$ and by optical activity $\theta(r_1) - \theta(r_2)$ of crystals of proteins of the blood plasma.

Experimentally, this information can be obtained using the method of polarization–phase filtration [23, 24]. Here, the object ($\{D\}$) is placed between two crossed phase filters, quarter-wave plates $\left(\{\Phi_1\} = \begin{Vmatrix} 1 & 0 \\ 0 & i \end{Vmatrix}, \quad \{\Phi_2\} = \begin{Vmatrix} i & 0 \\ 0 & 1 \end{Vmatrix}\right)$ and polarizers $\left(\{P_1\} = \begin{Vmatrix} 1 & 1 \\ 1 & 1 \end{Vmatrix}; \{P_2\} = \begin{Vmatrix} 1 & -1 \\ -1 & 1 \end{Vmatrix}\right)$ the transmission planes of which make angles of $+45°$ and $-45°$ with the fast axes. Analytically, the process of this polarization–phase filtration is described by the matrix equation

$$E = 0.5\{P_2\}\{\Phi_2\}\{D\}\{\Phi_1\}\{P_1\}E_0. \quad (9)$$

From (9), we obtain the following expression for the intensity of the transmitted radiation:

$$I = EE^* = (1 - \theta)^2 \delta^2. \quad (10)$$

As can be seen, the value of the intensity of points of the polarization filtered (relation (10)) laser image of the blood-plasma film proves to be functional $I(\delta, \theta)$.

From the medical point of view, for the diagnostics of the occurrence and differentiation of the type of a pathological process, independent information on changes in the concentration of albumin and globulin is important. To separate the components of linear birefringence δ of large-scale albumin crystals and

optical activity θ of small-scale globulin crystals, we used the method of spatial-frequency Fourier filtration of distributions of complex amplitudes of the laser-radiation field [39]. At the expense of a difference in the modulation periods of Fourier transforms of these structures in the frequency plane, one can select them using a vignetting (transparent or opaque) diaphragm.

Partial distributions of the complex amplitudes $\hat{E}(\delta)$ and $\dot{E}(\theta)$ of the laser image of a blood plasma layer can be restored using optical realization of the inverse Fourier transformation. Based on recorded intensity distributions, using (10), one determines corresponding phase distributions formed by the linear birefringence and optical-activity mechanisms,

$$\delta(x, y) \approx \sqrt{I(\delta, x, y)}, \quad (11)$$

$$\theta(x, y) \approx \sqrt{I(\theta, x, y)}. \quad (12)$$

Using relations (10)–(12), we obtain expressions for the modulus of DLCA for laser images of albumin and globulin polycrystalline networks filtered in spatial frequency,

$$|\mu(\delta, r_1, r_2)| \approx (1 + 2\Delta\delta_{12})^{-1}, \quad (13)$$

$$|\mu(\theta, r_1, r_2)| \approx (1 + 2\Delta\theta_{12})^{-1}. \quad (14)$$

INVESTIGATION TECHNIQUE AND ALGORITHMS OF DATA PROCESSING

Experimental investigations of DLCA coordinate distributions were performed using a Fourier polarimeter [40–43] (Fig. 1).

Blood-plasma layers (smears) were illuminated by a parallel beam with a diameter of 10 mm of He–Ne laser *1* ($\lambda = 0.6328$ μm). The transmission plane of polarizer *4* and the fast axis of quarter-wave plate *5* made angle $\Theta = 45°$.

Smears of blood plasma on optically homogeneous glass *6* were placed in the focal plane of polarization microobjective *7* (with a numerical aperture of 0.1, a focal distance of 30 mm, and a magnification of 4×). In the back focal plane, vignetting diaphragm *8* was placed. Polarization microobjective *9* (with a numerical aperture of 0.1, a focal distance of 30 mm, and a magnification of 4×) was arranged such that its focus coincided with the frequency plane of microobjective *7* and realized an inverse Fourier transform of a polarization filtered laser-radiation field. The coordinate distribution of the intensity of this field was recorded in the plane of a light-sensitive matrix of CCD camera *12* ($m \times n = 600 \times 800$ pixels), which was placed at a focal distance of microobjective *9*. CCD camera *12* ensured the measurement range of structural elements of the restored image of the blood-plasma layer from 2 to 2000 μm and made it possible to measure intensity distributions $I_\delta(m \times n)$ and $I_\theta(m \times n)$. Then, coordi-
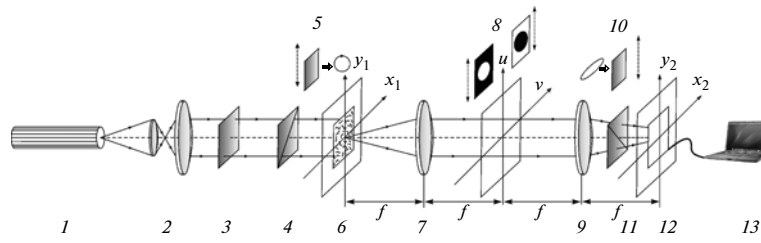
Fig. 1. Optical scheme of a Fourier polarimeter: (*1*) He–Ne laser, (*2*) collimator, (*3*) fixed quarter-wave plate, (*5, 10*) rotary quarter-wave plates, (*4, 11*) polarizer and analyzer, (*6*) biological specimen under investigation, (*7, 9*) polarization microobjectives, (*8*) vignetting diaphragm, (*12*) CCD camera, and (*13*) computer.

nate distributions $\delta(m \times n)$ and $\theta(m \times n)$ were calculated, which were scanned with a step of Δr of one pixel along the rows

$$\begin{pmatrix} r_{11} & r_{11} + \Delta r & \dots & r_{1m} \\ \downarrow & & & \downarrow \\ \rightarrow & \rightarrow & \rightarrow & \rightarrow \\ \downarrow & & & \downarrow \\ r_{n1} & r_{n1} + \Delta r & \dots & r_{nm} \end{pmatrix}.$$

For each pair of points $(r_{ik}, r_{ik} + \Delta r)$, using relations (13) and (14), DLCA moduli $\mu_\delta(r_{ik}, r_{ik} + \Delta r)$ and $\mu_\theta(r_{ik}, r_{ik} + \Delta r)$ were determined.

As a result, we found the coordinate distributions

$$\mu_{\delta,\theta} \begin{pmatrix} (r_{11}; r_{11} + \Delta r) & \dots & (r_{1m-1}, r_{1m-1} + \Delta r) \\ \dots & \dots & \dots \\ (r_{n1}, r_{n1} + \Delta r) & \dots & (r_{nm-1}, r_{nm-1} + \Delta r) \end{pmatrix}$$

of the images of blood-plasma films.

To objectively determine these distributions, we used complex statistical correlation and fractal analyses. Set of statistical moments of the first to fourth orders $Z^\mu_{j=1,2,3,4}$ was calculated from the following relations [25, 28]:

$$Z^\mu_1 = \frac{1}{N}\sum_{i=1}^{N}|\mu_i|, \quad Z^\mu_2 = \sqrt{\frac{1}{N}\sum_{i=1}^{N}\mu_i^2},$$

$$Z^\mu_3 = \frac{1}{(Z^\mu_2)^3}\frac{1}{N}\sum_{i=1}^{N}\mu_i^3, \quad Z^\mu_4 = \frac{1}{(Z^\mu_2)^4}\frac{1}{N}\sum_{i=1}^{N}\mu_i^4. \quad (15)$$

Here, N is the number of pixels of the digital camera. Correlation analysis of DLCA distributions is based on the autocorrelation method using the function [40]

$$K^\mu_{i=1-n}(\Delta m) = \lim_{m \to 0}\frac{1}{m}\int_1^m [\mu(m)][\mu(m - \Delta m)]dm. \quad (16)$$

Here, Δm is the step of one pixel with which the coordinates $(x = 1-m)$ of the DLCA distribution for the ith row of pixels of the digital camera are varied.

The resulting expression for the autocorrelation function was obtained by averaging of partial functions over all the rows $i = 1-n$,

$$K^\mu(\Delta m) = \frac{\sum_{i=1}^{n}K^\mu_i(\Delta m)}{n}. \quad (17)$$

To quantitatively characterize autocorrelation dependences $K^\mu(\Delta m)$, we used "correlation moment" Q^μ_4, which determines their excess,

$$Q = \frac{\sum_{i=1}^{N}(K(\Delta m))_i^4}{\left(\sum_{i=1}^{N}(K(\Delta m))_i^2\right)^2}. \quad (18)$$

Fractal analysis [14, 28, 43] of distributions $\mu(m \times n)$ was based on calculation of logarithmic dependences $\log J(\mu) - \log d^{-1}$ of power spectra $J(\mu)$, where $\nu = d^{-1}$ are spatial frequencies, which are determined by geometric dimensions d of structural elements of the laser image of a blood-plasma layer. All distributions $\log J(\mu) - \log d^{-1}$ were characterized by the dispersion

$$D^\mu = \sqrt{\frac{1}{N}\sum_{i=1}^{N}[\log J(\mu) - \log d^{-1}]_i^2}. \quad (19)$$

To classify distributions $\mu(m \times n)$, dependences $\log J(\mu) - \log d^{-1}$ were approximated by the least-squares method by curves $V(\eta)$ of the following types:

• $\mu(m \times n)$ —fractal or scale-self-similar if there was a constant slope angle η within two to three decades of variation of dimension d;

• $\mu(m \times n)$—multifractal if there were several slope angles η; and

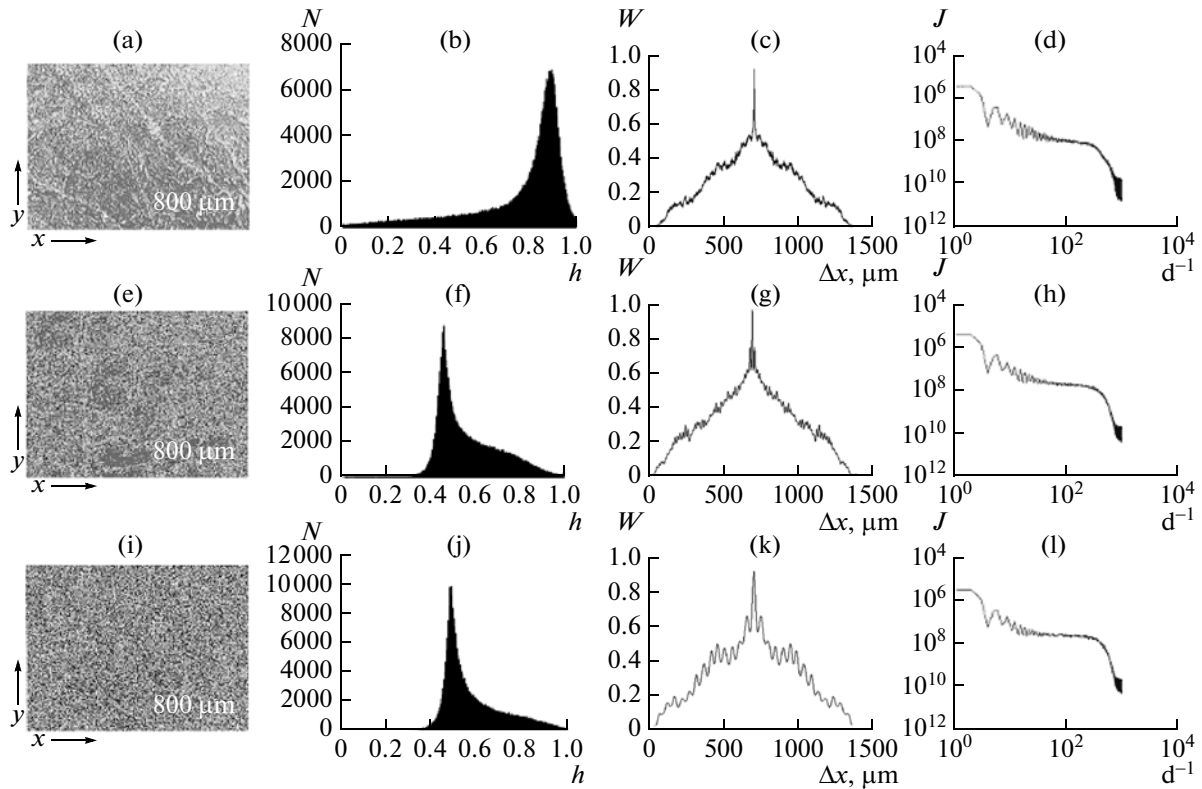• $\mu(m \times n)$ —random if there were no stable slope angles η.

Fig. 2. (a, e, i) Coordinate structure, (b, f, j) histograms $N(h)$, (c, g, k) autocorrelation functions W, and (d, h, l) logarithmic dependences of power spectra of DLCA distributions for images of blood-plasma films of patients of (a–d) group 1, (e–h) group 2, and (i–l) group 3.

EXPERIMENTAL RESULTS AND DISCUSSION

As the object of investigation, we used three groups of optically thin (geometric thickness 15–20 μm; extinction coefficient $\tau \approx 0.077$–0.084) blood-plasma layers taken from patients with the following diagnoses:

• group 1—healthy patients (donors)—23 specimens;

• group 2—rheumatoid-arthritis patients (inflammatory process)—22 specimens; and

• group 3—breast-cancer patients—19 specimens.The diagnostic possibilities of complex polarization–phase and spatial frequency processing of laser images of blood-plasma films are illustrated by the dependences presented in Figs. 2–4. Comparative analysis of histograms (b, f, j), autocorrelation functions (c, g, l), and logarithmic dependences of power spectra (d, h, m) of distributions $|\mu(r_1, r_2)|$ revealed significant differences between the control group and groups 2 and 3. Statistically, these differences manifest themselves in transformation of histograms of DLCA distributions of laser images of plasma films (Figs. 2b, 2f, 2j). As is seen, histograms $|\mu(r_1, r_2)|$ of images of blood-plasma films taken from healthy patients are characterized by localization of the main extremum in

the range of maximal values of DLCA. This indicates that phase fluctuations introduced by the polycrystalline network of blood-plasma proteins are rather weak, as a result of which $|\mu(r_1, r_2)| \rightarrow 1$.

Pathological states (groups 2 and 3) are characterized by an increase in the birefringence of polycrystalline networks—first of all, due to an increase in the concentration of globulin [35]. Therefore, an increase in the phase modulation leads to a shift of extrema of histograms (Figs. 2f, 2j) to the range of smaller values

Table 1. Parameters P of statistical, correlation, and self-similar structures of coordinate DLCA distributions for laser images of polycrystalline networks of proteins of blood plasma

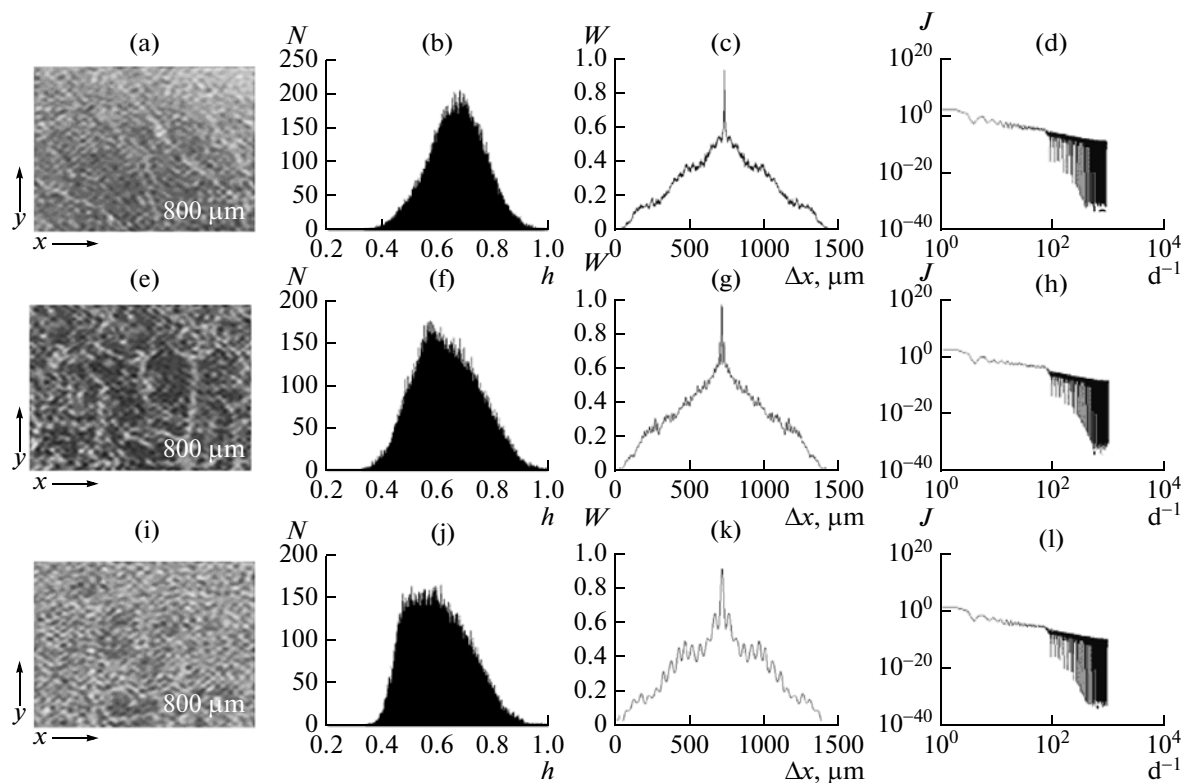| P	Group 1	Group 2	Group 3
Z_1	0.85 ± 0.13	0.44 ± 0.06	0.42 ± 0.06
Z_2	0.16 ± 0.02	0.14 ± 0.02	0.13 ± 0.02
Z_3	2.77 ± 0.44	1.54 ± 0.26	1.41 ± 0.19
Z_4	1.08 ± 0.15	2.2 ± 0.3	2.42 ± 0.38
Q_4	0.24 ± 0.04	1.15 ± 0.19	1.38 ± 0.23
$V(\eta)$	Fractal	Random	Random
D	0.23 ± 0.03	0.26 ± 0.03	0.28 ± 0.04

Fig. 3. (a, e, i) Coordinate structure, (b, f, j) histograms $N(h)$, (c, g, k) autocorrelation functions W, and (d, h, l) logarithmic dependences of power spectra of DLCA distributions $|\mu(\delta, r_1, r_2)|$ of points of spatial-frequency filtered laser images of a large-scale polycrystalline albumin network of blood-plasma layers of patients of (a–d) group 1, (e–h) group 2, and (i–l) group 3.

of DLCA ($|\mu(r_1, r_2)| \to 0.5$). In addition, autocorrelation functions $K^\mu(\Delta m)$ of coordinate distributions $\mu(m \times n)$ (Figs. 2g, 2l) decay more rapidly. This fact also indicates an increase in the phase inhomogeneity of the laser images of blood-plasma films for rheumatoid-arthritis patients (group 2) and breast-cancer patients (group 3). In addition, random coordinate distributions $\mu(m \times n)$ are formed. This fact follows from the absence of a stable slope of approximating curves $V(\eta)$ (Figs. 2d, 2h, 2l). At the same time, differentiation of the type and degree of severity of the pathological state (inflammatory process (Figs. 2f–2h) or cancer (Figs. 2i–2l)) is barely possible (Table 1).

Results of the method of spatial-frequency large-scale Fourier selection of phase laser images of specimens of all the groups are illustrated by the dependences presented in Fig. 3. Comparative analysis of the set of parameters that characterize coordinate distributions $|\mu(\delta, r_1, r_2)|$ revealed certain differences between them. Namely, histograms of the distribution of values of DLCA of the laser images of blood-plasma films taken from patients of groups 2 and 3 are characterized by an asymmetric shape with respect to the main extremum (Figs. 3f, 3j) compared to the similar distribution that was determined for a specimen of blood

plasma taken from a healthy donor (Fig. 3b). In our opinion, the revealed feature is related to a certain increase in the concentration not only of globulin, but also of albumin, in the blood plasma of diseased patients. As a result of this biochemical process, the level of linear birefringence and corresponding phase modulation $\delta(m \times n)$ increase. Therefore, small values of DLCA become more probable in histograms $|\mu(\delta, r_1, r_2)|$. For a more severe pathological process (cancer), the degree of asymmetry increases (Figs. 3f, 3j).

Dependences of autocorrelation functions of DLCA distributions for laser images of large-scale component of polycrystalline networks of blood-plasma films decrease smoothly and monotonically (Figs. 3c, 3g, 3k). This fact indicates that the structure of corresponding coordinate distributions $|\mu(\delta, r_1, r_2)|$ is rather homogeneous. In addition, a scale-self-similar shape of these distributions was revealed; i.e., logarithmic dependences of power spectra of distributions $|\mu(\delta, r_1, r_2)|$ are characterized by the same slope angle in almost the entire range of change of geometric dimensions, from 2 to 1000 μm (Figs. 3d, 3h, 3l) [15].

Therefore, "asymmetrization" of histograms of DLCA distributions $|\mu(\delta, r_1, r_2)|$ proved to be the main
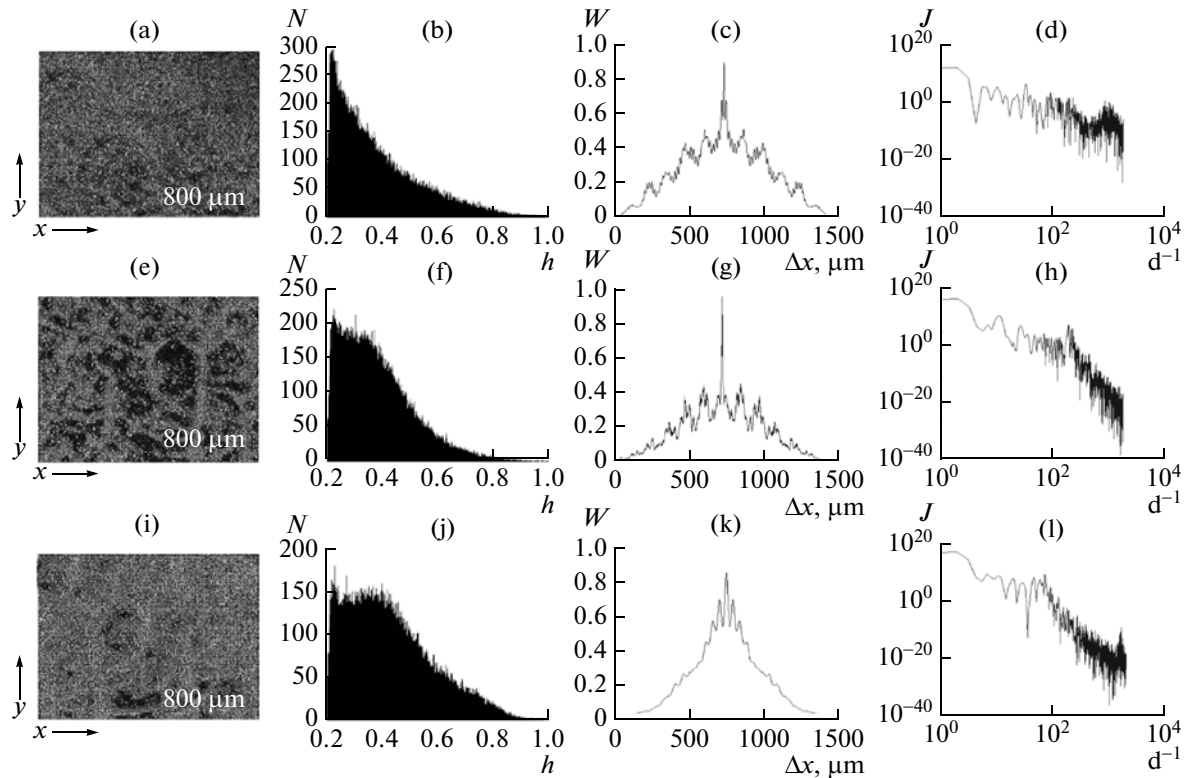
Fig. 4. (a, e, i) Coordinate structure, (b, f, j) histograms $N(h)$, (c, g, k) autocorrelation functions W, and (d, h, l) logarithmic dependences of power spectra of DLCA distributions $|\mu(\theta, r_1, r_2)|$ of points of spatial-frequency filtered laser images of a small-scale polycrystalline globulin network of blood-plasma layers of patients of (a–d) group 1, (e–h) group 2, and (i–l) group 3.

criterion for differentiation of inflammatory and oncological changes in the human organism.

A different pattern is observed in complex statistical, correlation, and fractal analyses of spatial-frequency filtered coordinate distributions of DLCA for laser images of small-scale optically active globulin networks of blood-plasma films (Fig. 4).

Comparison of the obtained results (Fig. 4) revealed the following polarization–correlation signs

of the occurrence of a pathological process. First, there is a substantial increase in the probability of finding the magnitudes of DLCA of laser images for specimens of groups 2 and 3 in the range of minimal values, $0 \leq \mu_\theta \leq 0.35$ (Figs. 4f, 3j). Second, a "pathological" increase in the influence of the optical activity of blood-plasma films leads to the formation of randomly arranged centers of phase modulation. Correlatively, this process manifests itself in a more rapid decrease (narrowing of the half-width) in corresponding auto-

Table 2. Parameters P of statistical, correlation, and self-similar structures of coordinate DLCA distributions for laser images of polycrystalline networks of proteins of blood-plasma films

P	μ_δ			μ_θ		
	group 1	group 2	group 3	group 1	group 2	group 3
Z_1	0.63 ± 0.11	0.59 ± 0.09	0.55 ± 0.008	0.11 ± 0.01	0.15 ± 0.03	0.25 ± 0.03
Z_2	0.27 ± 0.05	0.25 ± 0.04	0.22 ± 0.02	0.09 ± 0.01	0.14 ± 0.03	0.23 ± 0.037
Z_3	0.07 ± 0.01	0.41 ± 0.07	2.11 ± 0.37	2.23 ± 0.31	1.11 ± 0.17	0.53 ± 0.12
Z_4	0.08 ± 0.01	0.17 ± 0.03	0.22 ± 0.03	1.56 ± 0.27	0.85 ± 0.12	0.41 ± 0.075
Q_4	0.040 ± 0.007	0.05 ± 0.01	0.055 ± 0.73	1.14 ± 0.19	2.45 ± 0.29	4.05 ± 0.61
$V(\eta)$	Fractal	Fractal	Fractal	Random	Random	Random
D	0.32 ± 0.05	0.29 ± 0.04	0.27 ± 0.04	0.14 ± 0.02	0.11 ± 0.02	0.13 ± 0.02

correlation dependences (Figs. 4g, 4l). We note that these signs are most pronounced for breast cancer.

Quantitatively, differences between coordinate distributions of DLCA parameters for laser images of networks of blood-plasma films with linear birefringence μ_δ and optical activity μ_θ are illustrated by the data presented in Table 2. Comparative analysis of the obtained results revealed the following parameters that are efficient in diagnostics and differentiation of different pathological states (highlighted in gray).

• For the three groups considered, the third statistical moment, Z_3, which characterizes distributions μ_δ of laser images of linearly birefringent albumin crystals, differs from five- to sixfold.

• The complete set of statistical moments, $Z_{i=1;2;3;4}$, of distributions μ_θ for laser images of the network of optically active globulin crystals shows a range of intergroup differences from 1.5- to 4-fold.

• The correlation moment of the fourth order, Q_4, of autocorrelation functions of distributions μ_θ shows a range of intergroup differences from 2.1- to 3.6-fold.

CONCLUSIONS

We have proposed and analytically substantiated a method of correlation−phase analysis of laser images of polycrystalline networks of weakly anisotropic blood-plasma films with spatial-frequency filtration of manifestations of linear birefringence and optical activity of albumin and globulin.

We have performed comparative investigations of the efficiency of the developed method in diagnostics of occurrence and differentiation of the degree of severity (inflammatory process−cancer) of a pathological state of the human organism.

We have determined criteria of differentiation of rheumatoid arthritis and breast cancer based on statistical, correlation, and fractal analyses of spatial-frequency filtered DLCA distributions of laser images of polycrystalline albumin−globulin networks.

REFERENCES

1. V. V. Tuchin, Usp. Fiz. Nauk **167**, 517 (1997).
2. X. Wang and G. Yao, Appl. Opt. **41**, 792 (2002).
3. X. Wang and L.-H. Wang, J. Biomed. Opt. **7**, 279 (2002).
4. X. Wang, L. Wang, C.-W. Sun, and C. C. Yang, J. Biomed. Opt. **8**, 608 (2003).
5. A. Yu. Seteikin, Russ. Phys. J. **48** (3), 53 (2005).
6. J. F. de Boer, T. E. Milner, M. G. Ducros, S. M. Srinivas, and J. S. Nelson, in *Handbook of Optical Coherence Tomography* (2002), pp. 237−274.
7. S. Jiao, M. Todorovic, G. Stoica, and L. V. Wang, Appl. Opt. **44**, 5463 (2005).
8. S. Makita, Y. Yasuno, T. Endo, M. Itoh, and T. Yatagai, Opt. Review **12**, 146 (2005).
9. S. Makita, Y. Yasuno, T. Endo, M. Itoh, and T. Yatagai, Appl. Opt. **45**, 1142 (2006).
10. M. C. Pierce, J. Strasswimmer, B. H. Park, B. Cense, and J. F. de Boer, J. Biomed. Opt. **9**, 287 (2004).
11. Y. Yasuno, S. Makita, Y. Sutoh, M. Itoh, and T. Yatagai, Opt. Lett. **27**, 1803 (2002).
12. M. C. Pierce, J. Strasswimmer, B. H. Park, B. Cense, and J. F. de Boer, J. Biomed. Opt. **9**, 287 (2004).
13. A. G. Ushenko, Opt. Spectrosk. **91** (2), 313 (2001).
14. O. V. Angel'skii, A. G. Ushenko, A. D. Arkhelyuk, S. B. Ermolenko, and D. N. Burkovets, Opt. Spectrosk. **88** (3), 444 (2000).
15. A. G. Ushenko, Opt. Spectrosk. **89** (4), 597 (2000).
16. V. Pishak, A. Ushenko, P. Gryhoryshyn, S. Yermolenko, V. Rudeychuk, and O. Pishak, Proc. SPIE—Int. Soc. Opt. Eng. **3317**, 418 (1997).
17. O. V. Angelsky, Yu. Ya. Tomka, A. G. Ushenko, Ye. G. Ushenko, and Yu. A. Ushenko, J. Phys. D: Appl. Phys. **38** (23), 4227 (2005).
18. F. Gori, M. Santarsiero, S. Vicalvi, R. Borghi, and G. Guattari, Pure Appl. Opt., No. 7, 941 (1998).
19. E. Wolf, Phys. Lett. A **312**, 263 (2003).
20. J. Tervo, T. Setala, and A. Friberg, Opt. Express **11**, 1137 (2003).
21. J. Ellis and A. Dogariu, Opt. Lett. **29**, 536 (2004).
22. O. V. Angelsky, A. G. Ushenko, and Y. G. Ushenko, Biomed. Opt. **10** (6), 060502 (2005).
23. Y. O. Ushenko, Y. Ya. Tomka, I. Z. Misevitch, V. V. Istratiy, and O. I. Telenga, Opt. Eng. **50**, 039001 (2011).
24. O. V. Angelsky, A. Ya. Bekshaev, P. P. Maksimyak, A. P. Maksimyak, S. G. Hanson, and C. Yu. Zenkova, Opt. Express **20**, 3563 (2012).
25. Yu. A. Ushenko, Yu. Ya. Tomka, and A. V. Dubolazov, Opt. Spectrosk.**110** (5), 814 (2011).
26. A. G. Ushenko, I. Z. Misevich, V. Istratiy, I. Bachyns'ka, A. P. Peresunko, O. K. Numan, and T. G. Moiysuk, Adv. Optical Technol., No. 423145 (2010).
27. S. H. Guminetskiy, A. G. Ushenko, I. P. Polyanskiy, A. V. Motrych, and F. V. Grynchuk, Proc. SPIE—Int. Soc. Opt. Eng. **7008**, 7008 27 (2008).
28. S. Yermolenko, A. Ushenko, P. Ivashko, F. Goudail, I. Gruia, C. Gavrila, D. Zimnyakov, and A. Mikhailova, Proc. SPIE—Int. Soc. Opt. Eng. **7388**, 73881 (2009).
29. A. Ushenko, S. Yermolenko, A. Prydij, S. Guminetsky, I. Gruia, O. Toma, and K. Vladychenko, Proc. SPIE—Int. Soc. Opt. Eng. **7008**, 7008 2 (2008).
30. Ming Lei and Baoli Yao, J. Biomed. Opt. **13**, 044024 (2008).
31. A. C. Curry, M. Crow, and A. Wax, J. Biomed. Opt. **13**, 014022 (2008).
32. T. D. Yang, W. Choi, T. H. Yoon, K. J. Lee, J.-S. Lee, et al., J. Biomed. Opt. **17**, 128003 (2012).
33. H. Deyhle, T. Weitkamp, S. Lang, G. Schulz, A. Rack, et al., Proc. SPIE—Int. Soc. Opt. Eng. **8506**, 85060 (2012).

34. O. V. Angel'skii, A. G. Ushenko, A. D. Arkhelyuk, S. B. Ermolenko, D. N. Burkovets, and Yu. A. Ushenko, Opt. Spectrosk. **89** (6), 973 (2000).

35. O. V. Angelsky, A. G. Ushenko, Y. G. Ushenko, and Y. Y. Tomka, J. Biomed. Opt. **11** (5), 054030 (2006).

36. O. V. Angelsky, A. G. Ushenko, Yu. A. Ushenko, and Ye. G. Ushenko, J. Phys. D: Appl. Phys. **39** (16), 3547 (2006).

37. A. G. Ushenko, Opt. Spectrosk. **91** (6), 937 (2001).

38. O. V. Angelsky, P. P. Maksimyak, and S. Hanson, *The Use of Optical Correlation Techniques for Characterizing Scattering Object and Media* (SPIE Press, Bellingham, 1999).

39. J. W. Goodman, *Laser Speckle and Related Phenomena*, Ed. by J. C. Dainty (Springer, Berlin, 1975).

40. A. G. Ushenko, Opt. Spectrosk. **91** (6), 932 (2001).

41. O. V. Angelsky, A. G. Ushenko, Yu. A. Ushenko, Ye. G. Ushenko, Yu. Ya. Tomka, and V. P. Pishak, J. Biomed. Opt. **10** (6), 060502 (2005).

42. O. V. Angel'skii, O. G. Ushenko, D. N. Burkovets, O. D. Arkhelyuk, and Yu. A. Ushenko, Laser Phys. **10** (5), 1136 (2000).

43. O. V. Angel'skii, A. G. Ushenko, A. D. Arkhelyuk, S. B. Ermolenko, and D. N. Burkovets, Quantum Electron. **29** (12), 1074 (1999).

Translated by V. Rogovoi